Physics Letters A 374 (2010) 4675–4677

Contents lists available at ScienceDirect

Physics Letters A

www.elsevier.com/locate/pla

Plasma focus based flash hard X-ray source in the 100 keV region with reproducible spectrum

V. Raspa *, P. Knoblauch, F. Di Lorenzo, C. Moreno

Departamento de Física, FCEyN-UBA, PLADEMA-CNEA and INFIP-CONICET, Pab. 1, Ciudad Universitaria, (1428) Buenos Aires, Argentina

ARTICLE INFO

Article history:
Received 14 May 2010
Received in revised form 24 July 2010
Accepted 15 September 2010
Available online 18 September 2010
Communicated by F. Porcelli

Keywords:
Plasma focus hard X-rays
Flash hard X-ray source
Flash radiography
Single shot HXR spectral analysis

ABSTRACT

A pulsed hard X-ray source with shot to shot reproducible spectrum, based on a 4.7 kJ small-chamber Mather-type plasma focus device, is presented. The hard X-ray output spectrum was measured in a single shot basis by differential absorption on metallic plates. The measured spectra have a single dominant peak around 75 keV and a spectral bandwidth covering the 40–150 keV range. A hard X-ray dose of (53 ± 3) μGy per shot was measured on axis at 53 cm from the source, and found to be uniform within a half aperture angle of 6°.

1. Introduction

Plasma focus technology offers pulsed X-ray sources of unmatched characteristics. Very high brightness, extremely short pulse duration, spectral richness, profuse emissions at very short wavelengths, cost effectiveness and simplicity of use and maintenance, are among their distinctive characteristics. Plasma focus devices were intensively investigated and used as outstanding X-ray sources for lithography [1–11], backlighting [12,13], micromachining [6] and radiography [14–28]. Applications field expands as more intense, energetic and stable X-ray sources are made available.

In the current Letter, we present a small plasma focus device whose hard X-ray output exhibits a shot to shot reproducible spectra that includes significative components beyond 100 keV ($\lambda < 12$ pm) and whose brightness is high enough to allow for introspective imaging of metallic objects. As an example, in Fig. 1, a single shot radiography of a standard door lock, mainly made on steel and brass, is shown.

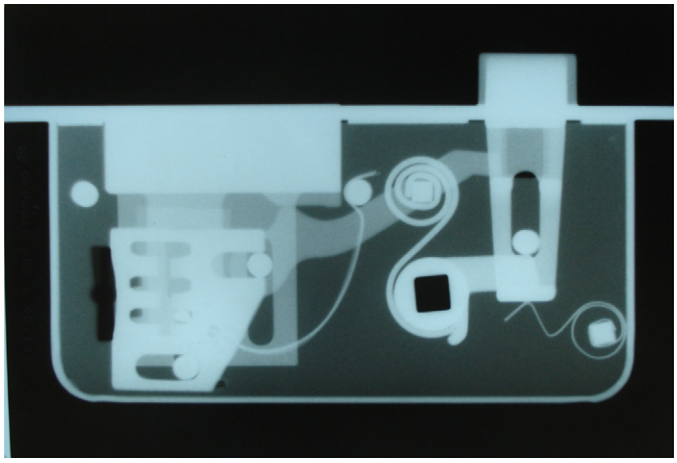

Fig. 1. Single shot radiography of a standard door lock made on steel and brass. Exposure time: 50 ns FWHM.

2. Material and methods

2.1. The device

A small-chamber Mather-type plasma focus device was adapted to function as a flash hard X-ray source of reproducible spectrum. The facility is powered by a capacitor bank, formed by fifteen Maxwell capacitors model 31161 (0.7 μF each) connected in parallel and charged up to 30 kV (4.7 kJ of stored energy), that delivers a peak current of 340 kA in a quarter of period of 1.23 μs. To reduce connection impedances, the capacitors were connected to the discharge chamber using 15 coaxial cables of 1 m in length and 19.8 Ω of characteristic impedance, and grouped in three identical modules, each of which is controlled by a spark gap switch from Maxwell, model 40264. An auxiliary, low inductance spark gap controlled by an external trigger, is used to simultaneously switch

* Corresponding author. Tel.: +54 11 4576 3371 ext. 122; fax: +54 11 4576 3357.
E-mail address: raspa@df.uba.ar (V. Raspa).

0375-9601/$ – see front matter
doi:10.1016/j.physleta.2010.09.023

the three main spark gaps, ensuring the discharge synchronicity within 10 ns. The overall bank stray inductance and resistance were measured in (55.6 ± 0.2) nH and (11.2 ± 0.1) mΩ, respectively. The capacitor bank footprint and height are 0.60 m^2 and 1 m, respectively. The coaxial electrodes are formed by a hollow copper anode (central electrode) surrounded by a squirrel-cage-like bronze cathode. They are separated by a Pyrex insulator and located coaxially inside a 1 dm^3 stainless steel cylindrical chamber of 2 mm thick lateral wall. The anode is a tube of 38 mm outer diameter, 2 mm thick wall, and 85 mm in length. The anode base, which is the target for the electron beam emitted as a consequence of the focalization, is made of lead and it is 2 cm thick. The cathode is formed by eight brass rods, each one of 3 mm in diameter and 87 mm in length, located equally spaced around a circle of 37 mm in radius concentric with the anode. The insulator sleeve is 50 mm in outer diameter, 4 mm thick wall, and 34 mm in length. Insulator walls thinner than 3 mm are not advisable because they break after a few hundreds of shots. The insulator length was chosen according to criteria given in Ref. [29]. The discharge chamber is filled with 3.5 mbar of an admixture of 2.5% (in volume) of argon in deuterium, since it maximizes the hard X-ray production and the shot to shot regularity for this device. The output window for the hard X-ray radiation is a 0.75 mm thick stainless steel flat disk, which is also the front end of the chamber, and it is placed at 14 cm from the electron beam target.

A non-integrating Rogowski coil and a photomultiplier tube coupled to a cylindrical NE102A plastic scintillator 5 cm thick and 5 cm in diameter were used to monitor the discharge and the hard X-ray output, respectively. The photomultiplier signal exhibits a typical FWHM of 50 ns for the X-ray pulses. High sensitivity KODAK T-Mat/G X-ray film along with terbium-doped gadolinium oxysulphide (Gd_2O_2S:Tb) intensifying screens were used as hard X-ray detector.

2.2. Spectral measurements

A method based on differential absorption on metallic plates and the densitometry of their radiographs [30], was used to measure the continuum component of the hard X-ray output spectrum. Such method can be briefly outlined as follows.

For a set of metallic samples made of different materials and thicknesses, transmission coefficients T_{ij} can be defined, as

$$T_{ij} \equiv \frac{\int_0^\infty \eta(E) S(E) e^{-k_i(E) d_{ij}}\, dE}{\int_0^\infty \eta(E) S(E)\, dE} \tag{1}$$

where $\eta(E)$ is the spectral response of the detector, $S(E)$ is the unknown hard X-ray spectrum and d_{ij} is the thickness of the sample j made of the material i. $k_i(E)$ is the linear attenuation coefficient that characterizes the radiation decay, depending on the sample material and the energy of the attenuated spectral component [31]. A standard regularization method [32] was followed to infer a point-defined function $S(E)$ from the transmission values prescribed by Eq. (1) and the corresponding measured values T_{ij}^{meas}.

To take eventual film inhomogeneities into account, the densitometric analysis of the radiographs was done by means of its normalized optical density (NOD), defined as the ratio between the optical density (OD) measured for the region of interest, and that measured for the corresponding nearby background. A calibration of the film exposure was conducted as in Ref. [30] to relate the NOD measurements with certified transmission values. Each T_{ij}^{meas} value was obtained interpolating the calibration data for the corresponding normalized optical density.

The used set of plates is detailed in Ref. [30], and a single shot radiograph of them, when placed at 70 cm from the chamber front wall, is shown in Fig. 2. To illustrate the NOD measurements, Fig. 3 shows the normalized optical density for the copper samples as a function of the sample thickness. All the processed radiographs verify that the film exposure was above the film fog level (which corresponds to OD = 0.2) and well below the saturation level (OD = 3.5) [33].

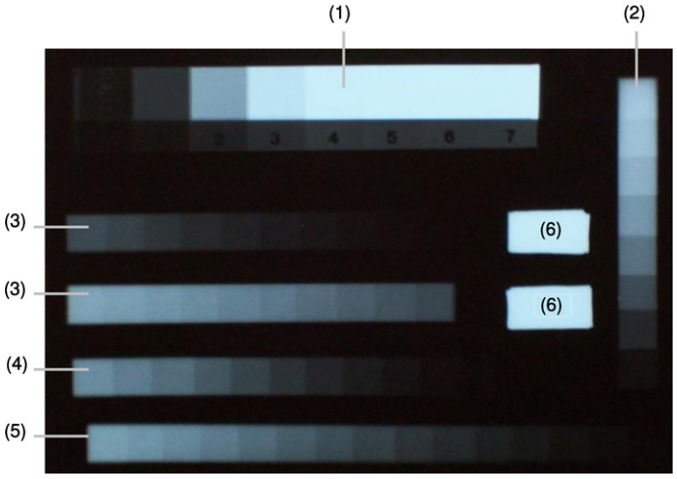

Fig. 2. Single-shot radiographic image of the plates set used to determine the radiation spectrum. Refs.: (1) calibration image, (2) silver, (3) nickel, (4) titanium, (5) copper and (6) fog level reference.

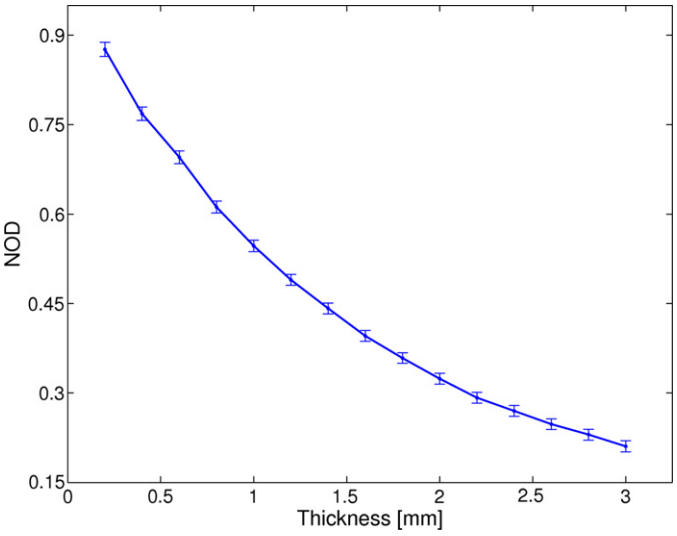

Fig. 3. Normalized optical density measured for the copper samples as a function of the sample thickness.

3. Results

Fig. 4 presents the hard X-ray output spectrum of single plasma focus shots fired under the same experimental conditions. As it can be observed, there are no substantial differences between the obtained spectra. All of them have a single dominant peak around 75 keV and a spectral bandwidth covering the 40–150 keV region. Moreover, the spectral amplitudes decay for increasing energies greater than 75 keV until becoming negligible beyond 250 keV. The small bump that appears at ∼ 25 keV is a numerical artifact of the regularization method. In fact, spectral components below 30 keV are strongly attenuated (more than 100 times) by the chamber front wall.

Since it is also very important for applications, the hard X-ray dose on axis was measured using thermoluminescent detectors

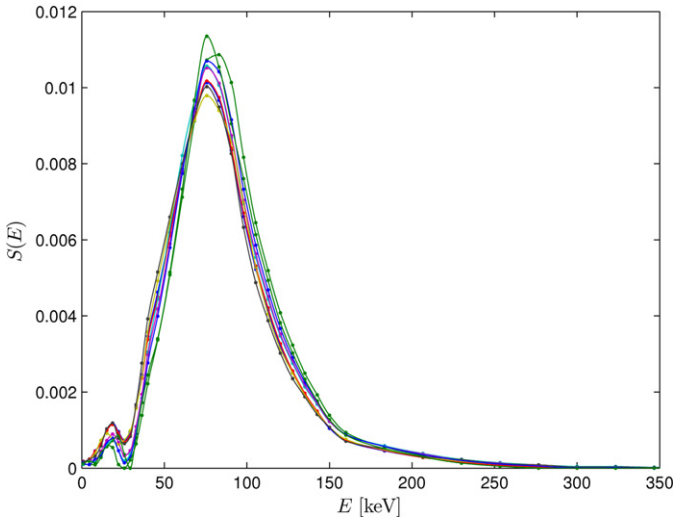

Fig. 4. Hard X-ray continuum spectra obtained from the analysis of different radiographies taken under the same experimental conditions.

Harshaw TLD 700 from Bicron, placed at 53 cm from the source. The TLDs were exposed to 40 shots to enhance the signal to noise ratio. An uniform irradiation (within ±5% of its mean value) over a disk of 5.6 cm in radius and an average dose value of (53 ± 3) μGy per shot over that area, were obtained from the measurements. This allows to estimate the half aperture angle of uniform dose for the beam in 6°.

Although the electron energy spectrum is unknown for our device, the hard X-ray dose mentioned in the preceding paragraph, was calculated using Monte Carlo simulations [34] in which the experimental setup was modeled and a monoenergetic beam of 100 keV electrons was assumed in the light of the obtained X-ray spectra.

The simulation gave a dose value of 136.8 mGy per coulomb deposited on the lead target. Thus, a deposited charge of 0.39 mC is required to reproduce the measured dose of 53 μGy. Considering that the X-ray emission lasts 50 ns, this allows to estimate an average current of 8 kA for the electron beam. Similarly, assuming monoenergetic electron beams either of 75 or 150 keV, average currents of 24 and 2 kA are obtained, respectively. This range of values is consistent with measurements previously reported [35–38] for plasma focus devices of stored energies and operating voltages similar to the one presented here.

4. Conclusions

A small chamber, medium energy, plasma focus device which is a pulsed hard X-ray source with reproducible spectrum in the 40–150 keV region, was presented. The method used to determine the hard X-ray spectrum allowed to test the spectral reproducibility of the hard X-ray output of a plasma focus device in this energy region, for the first time, in a single shot basis. The source is optimized for hard X-ray imaging applications, and is intense, energetic and wideband enough to be well suited for good contrast images of different metals. The metallic chamber window helps to strengthen the hard X-ray output spectrum without preventing radiographic applications on metallic objects.

Acknowledgements

This work was supported by UBA (Proj. X152), PLADEMA-CNEA and CONICET. C.M. is member of CONICET and P.K. is a Doctoral fellow of CONICET.

References

[1] Y. Kato, S.H. Be, Appl. Phys. Lett. 48 (1986) 686.
[2] Y. Kato, I. Ochiai, Y. Watanabe, S. Murayama, J. Vac. Sci. Technol. B 6 (1988) 195.
[3] E.P. Bogolyubov, V.D. Bochkov, V.A. Veretennikov, L.T. Vekhoreva, V.A. Gribkov, A.V. Dubrovskii, Y.P. Ivanov, A.I. Isakov, O.N. Krokhin, P. Lee, S. Lee, V.Ya. Nikulin, A. Serban, P.V. Silin, X. Feng, G.X. Zhang, Phys. Scr. 57 (1998) 488.
[4] S. Lee, P. Lee, G. Zhang, X. Feng, V. Gribkov, M. Liu, A. Serban, T. Wong, IEEE Trans. Plasma Sci. 26 (1998) 1119.
[5] A.V. Dubrovsky, V.A. Gribkov, Y.P. Ivanov, P. Lee, S. Lee, M. Liu, V.A. Samarin, Nukleonika 46 (2001) S107.
[6] V.A. Gribkov, A. Srivastava, P.L.C. Keat, V. Kudryashov, S. Lee, IEEE Trans. Plasma Sci. 30 (2002) 1331.
[7] R. Petr, A. Bykanov, J. Freshman, D. Reilly, J. Mangano, M. Roche, J. Dickenson, M. Burte, J. Heaton, Rev. Sci. Instrum. 75 (2004) 2551.
[8] D. Wong, A. Patran, T.L. Tan, R.S. Rawat, P. Lee, IEEE Trans. Plasma Sci. 32 (2004) 2227.
[9] D. Wong, T.L. Tan, P. Lee, R.S. Rawat, A. Patran, Microelectron. Eng. 83 (2006) 1912.
[10] V.A. Gribkov, M. Liu, P.C.K. Lee, S. Lee, A.M. Srivastava, Microlithographic Techniques in Integrated Circuit Fabrication II, vol. 4226, SPIE, 2000, p. 151.
[11] V. Gribkov, A. Dubrovsky, M. Scholz, S. Jednorog, L. Karpinski, K. Tomaszewski, M. Paduch, R. Miklaszewski, V.N. Pimenov, L.I. Ivanov, E.V. Dyomina, S.A. Maslyaev, M.A. Orlova, Nukleonika 51 (2006) 55.
[12] F.N. Beg, I. Ross, A. Lorenz, J.F. Worley, A.E. Dangor, M.G. Haines, J. Appl. Phys. 88 (2000) 3225.
[13] M. Zakaullah, K. Alamgir, M. Shafiq, M. Sharif, A. Waheed, IEEE Trans. Plasma Sci. 30 (2002) 2089.
[14] G. Decker, R. Wienecke, Physica B+C 82 (1976) 155.
[15] A.V. Dubrovsky, P.V. Silin, V.A. Gribkov, I.V. Volobuev, Nukleonika 45 (2000) 185.
[16] F. Castillo, M. Milanese, R. Moroso, J. Pouzo, M. Santiago, IEEE Trans. Plasma Sci. 29 (2001) 921.
[17] A. Da Re, F. Mezzetti, A. Tartari, G. Verri, L. Rapezzi, V.A. Gribkov, Nukleonika 46 (2001) S123.
[18] S. Hussain, S. Ahmad, M.Z. Khan, M. Zakaullah, A. Waheed, J. Fusion Energy 22 (2003) 195.
[19] S. Hussain, M. Zakaullah, S. Ali, S. Bhatti, A. Waheed, Phys. Lett. A 319 (2003) 181.
[20] S. Hussain, M. Zakaullah, S. Ali, A. Waheed, Plasma Sci. Technol. 6 (2004) 2296.
[21] S. Hussain, M. Shafiq, R. Ahmad, A. Waheed, M. Zakaullah, Plasma Sources Sci. Technol. 14 (2005) 61.
[22] C. Moreno, V. Raspa, L. Sigaut, R. Vieytes, A. Clausse, Appl. Phys. Lett. 89 (2006) 091502.
[23] A.V. Dubrovsky, V.A. Gribkov, Y.P. Ivanov, L. Karpiński, M. Orlova, V.M. Romanova, M. Scholz, I.V. Volobuev, Nukleonika 51 (2006) 21.
[24] F. Castillo, I. Gamboa-deBuen, J.J.E. Herrera, J. Rangel, S. Villalobos, Appl. Phys. Lett. 92 (2008) 051502.
[25] V. Raspa, F. Di Lorenzo, P. Knoblauch, A. Lazarte, A. Tartaglione, A. Clausse, C. Moreno, PMC Phys. A 2 (5) (2008), doi:10.1186/1754-0410-2-5.
[26] Ye.P. Bogolubov, M.V. Koltunov, B.D. Lemeshko, V.I. Mikerov, V.N. Samosyuk, P.P. Sidorov, D.I. Yurkov, Nucl. Instrum. Methods Phys. Res. Sect. A 605 (2009) 62.
[27] S. Hussain, High Efficiency X-Ray Source: Tailoring a Plasma Focus Device for Radiography, VDM Verlag, Saarbrücken, Germany, 2009.
[28] S. Hussain, M. Shafiq, M. Zakaullah, Appl. Phys. Lett. 96 (2010) 031501.
[29] F. Di Lorenzo, V. Raspa, P. Knoblauch, A. Lazarte, C. Moreno, A. Clausse, J. Appl. Phys. 102 (2007) 033304.
[30] V. Raspa, C. Moreno, Phys. Lett. A 373 (2009) 3659.
[31] J.H. Hubbell, S.M. Seltzer, X-Rays Mass Attenuation Coefficients, Ionizing Radiation Division, Physics Laboratory, NIST, Gaithersburg, MD, USA, 1996.
[32] W.H. Press, S.A. Teukolsky, W.T. Vetterling, B.P. Flannery, Numerical Recipes in C: The Art of Scientific Computing, Cambridge Univ. Press, New York, 1992.
[33] Eastman Kodak Company, KODAK T-MAT G/RA Film/4155, Datasheet, 1994.
[34] J.F. Briesmeister, MCNP – A general Monte Carlo code for neutron and photon transport, Rpt LA-7396-M, Rev. 2, Los Alamos National Laboratory, Los Alamos, NM, 1986.
[35] J.R. Smith, C.M. Luo, M.J. Rhee, R.F. Schneider, Phys. Fluids 28 (1985) 2305.
[36] A. Patran, L.C. Tan, D. Stoenescu, M.S. Rafique, R.S. Rawat, S.V. Springham, T.L. Tan, P. Lee, M. Zakaullah, S. Lee, Plasma Sources Sci. Technol. 14 (2005) 549.
[37] N.K. Neog, S.R. Mohanty, Phys. Lett. A 361 (2007) 377.
[38] T. Zhang, J. Lin, A. Patran, D. Wong, S.M. Hassan, S. Mahmood, T. White, T.L. Tan, S.V. Springham, S. Lee, P. Lee, R.S. Rawat, Plasma Sources Sci. Technol. 16 (2007) 250.